HHS Public Access

Author manuscript

J Neuroimmunol. Author manuscript; available in PMC 2017 March 15.

Published in final edited form as:

J Neuroimmunol. 2016 March 15; 292: 116–125. doi:10.1016/j.jneuroim.2016.01.022.

Characterization of neuropathology in the HIV-1 transgenic rat at different ages

William C Reid[1,*], **Wael G Ibrahim**[1,*], **Saejeong J. Kim**, **Frank Denaro**[3], **Rafael Casas**[1], **Dianne E Lee**[1], **Dragan Maric**[4], and **Dima A Hammoud**[1,†]

[1]Center for Infectious Disease Imaging (CIDI), Radiology and Imaging Sciences, Clinical Center, National Institutes of Health, Bethesda, Maryland, USA.

[2]Frank Laboratory, Radiology and Imaging Sciences, Clinical Center, National Institutes of Health, Bethesda, Maryland, USA

[3]Department of Biology, Morgan State University, Baltimore, Maryland, USA.

[4]Division of Intermural Research (DIR), National Institute of Neurological Disorders and Stroke (NINDS), National Institutes of Health, Bethesda, Maryland, USA.

Abstract

The transgenic HIV-1 rat (Tg) is a commonly used neuroHIV model with documented neurologic/behavioral deficits. Using immunofluorescent staining of the Tg brain, we found astrocytic dysfunction/damage, as well as dopaminergic neuronal loss/dysfunction, both of which worsening significantly in the striatum with age. We saw mild microglial activation in young Tg brains, but this decreased with age. There were no differences in neurogenesis potential suggesting a neurodegenerative rather than a neurodevelopmental process. Gp120 CSF levels exceeded serum gp120 levels in some animals, suggesting local viral protein production in the brain. Further probing of the pathophysiology underlying astrocytic injury in this model is warranted.

Graphical abstract

[†]Corresponding author: Dima A. Hammoud, MD, National Institutes of Health/Clinical Center, 10 Center Drive, Room 1C368, Bethesda, MD 20814-9692, Phone: 301-402-3041, Fax: 301-496-9933, hammoudd@cc.nih.gov.

[*]Authors contributed equally to this manuscript

The authors declare that they have no conflict of interest.

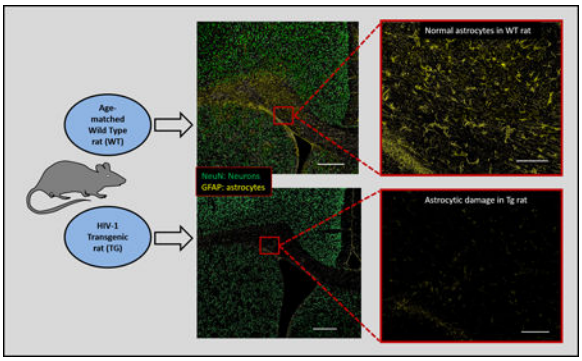

Keywords

Neuro-HIV; HIV-1 transgenic rat; viral proteins; neuropathology; astrocytic loss; neurotoxicity

1. INTRODUCTION

Since the introduction of anti-retroviral therapy (ART), the prevalence of HIV-associated dementia (HAD) decreased, however less fulminant forms of HIV-related neurological dysfunction became more common and currently affect around 52% of the HIV-positive (HIV+) patient population (McArthur et al., 2003, McArthur et al., 2010). The exact neuropathology leading to milder forms of HIV-associated neurocognitive disorders (HAND) is not fully understood but is probably multifactorial. Unlike microglia and astrocytes, neurons do not seem to get productively infected with HIV (Kovalevich and Langford, 2012). The neurologic damage is rather thought related to persistent low level neuroinflammation (Desplats et al., 2013), neurotoxic effects of viral proteins (Agrawal et al., 2012, Hu et al., 2009, Mocchetti et al., 2011), as well as the disruption of the supportive and neurotrophic role of astrocytes (Bezzi et al., 2001) and oligodendrocytes (Radja et al., 2003).

Short of using expensive and sentient SIV infected monkeys, or sophisticated humanized mice models, the HIV-1 transgenic (Tg) rat is used by many groups as an HIV model. This non-infectious rat model expresses 7 of the 9 HIV-1 viral proteins including gp120, nef and tat and is known to develop clinically relevant neuropathologies (Reid et al., 2001) and cognitive deficits (Lashomb et al., 2009, Moran et al., 2012, Moran et al., 2013a, Peng et al., 2010, Vigorito et al., 2007). It thus appears to be of particular importance and practicality for the evaluation of neurological HIV complications.

In this study, we wanted to better understand the pattern of neurotoxicity underlying the neurological and behavioral problems described in the commercially-available Tg rat. Towards this goal, we compared immunofluorescence staining of various neuronal and glial markers, dopaminergic function and neurogenesis potential between the Tg and WT rats, at different ages. We also measured the levels of gp120 (as a representative viral protein) in the cerebrospinal fluid (CSF) and compared to serum levels of Gp120.

2. MATERIALS AND METHODS

2.1. Animals

Male HIV-1 Tg rats (F344/Hsd) and male age-matched controls (F344, WT) were purchased from Harlan Inc. (Indianapolis, IN) and used in various experiments. We used a total number of 43 Tg and 34 WT rats in all the experiments, ranging in age from 1 to 20 months. Some of the animals used for non-terminal procedures (serum and CSF collection) were then re-used for the terminal procedures (ELISA of brain lysates, PCR and immunostaining). Animal care and all experimental procedures were approved by the Institutional Animal Care and Use Committee (IACUC) of the National Institutes of Health/ Clinical Center (NIH/CC).

2.2.Immunofluorescence Staining and Quantification

Rat brain sections were evaluated using immunofluorescence and compared in four groups of animals: 3 Tg and 3 WT one-month-old rats, 5 Tg and 3 WT three-month-old rats (total young: 8 Tg and 6 WT), 3 Tg and 2 WT seven-month-old and 3 Tg and 3 WT nine-month-old rats (total middle-aged: 6 Tg and 5 WT). The relevant slices were obtained from two areas of interest: striatum, bregma 0.48 to 0.12 millimeters (mm) and hippocampus, bregma −2.92 to −3.24 mm, as per the Paxinos and Watson atlas (The Rat Brain in Stereotaxic Coordinates, Sixth Edition, Academic Press, San Francisco, CA).

Multi-epitope immunolabeling protocols were applied to identify the cellular phenotypes in fresh frozen brain slices using different combinations of primary antibodies. The labeled targets included NeuN, GFAP, Iba1, tyrosine hydroxylase (TH) and proliferating cell nuclear antigen (PCNA). Each of the above primary immunoreactions was visualized using appropriate fluorophore-conjugated (Alexa Fluor dyes) secondary antibodies. The cell nuclei were counterstained using 1 ug/ml DAPI to facilitate cell counting.

Quantification of immunofluorescent staining was performed using FIJI image processing package, based on ImageJ (NIH, Bethesda, MD). The locations of the striatal and cortical ROIs were identical for all the animals. For NeuN, Iba1 and PCNA cell counts, the RGB bitmap images were converted to 8-bit grayscale and the threshold was adjusted to include only cells of interest and eliminate the background, and this was followed by counting, using the image based tool for counting nuclei plugin (ITCN). All images were processed using the same analysis parameters. The cell density (cells/mm2) was calculated from the total number of positive cells divided by the total area. For the staining intensity measurements of GFAP and TH also calculated for the total area (total intensity/mm2), the background fluorescent signal was removed by a thresholding process, visually selected by the user. The same cutoff value was then used to analyze all the slides stained concurrently.

Since our animal brains were stained in batches at different dates, we decided to use the ratios of staining instead of absolute measurement values to compare young and middle-aged animals. For each set of animals stained at the same time, we used the ratio of counts or the ratio of intensities of each Tg animal with respect to the corresponding co-stained WT rat(s). We then compared the individual animal ratios in the young (1–3 month-old) to those in the middle-aged (7–10 month-old) animals.

2.3. Viral protein analysis

2.3.1. Serum and CSF collection—Serum was collected from 28 Tg and 5 WT rats (age range: 3 to 20 month-old) by retro-orbital sampling, under anesthesia. We had CSF samples from 17 Tg rats (age range = 3 to 20 month-old), after excluding samples that were blood-tinged. Out of the latter, 13 rats had CSF and serum collected within a few days of each other.

For CSF collection, animals were first anesthetized and placed in a stereotaxic apparatus (Stoelting, Wood Dale, IL, USA), with their head positioned downward at around 45 degrees angle to their back and secured with ear bars. The back of the neck and base of skull were shaved and disinfected. The lower border of the skull was then palpated and a one inch, 30 Gauge needle attached to silicone tubing which ends in a 1cc Syringe was inserted horizontally, in a central location, between the occipital protuberance and the first cervical vertebra. The needle was then advanced slowly, with gentle negative pressure maintained within the syringe. Sometimes a slight change in the resistance upon puncturing the dura could be felt. As soon as the CSF was seen to flow into the silicone tubing, the needle was manually stabilized in place. Collection of CSF was then achieved by another operator pulling back the syringe plunger very slowly. The CSF was immediately placed into 0.5 ml Eppendorf tubes and frozen at −80 °C. The volume of CSF collected varied from 50 to 100 microliter. Some of the samples were minimally contaminated with blood and were included in the analysis. When the blood contamination was deemed to be significant, the sample was discarded. A total of 9 Tg rats had serum and CSF collections either on the same day or within a couple days from each other.

2.3.2. Brain lysate collection—We collected brain lysates from 7 Tg and 2 WT rats at different ages ranging from 2 to 20 month-old.

2.3.3. ELISA—Serum, CSF and brain lysate gp120 levels were quantified by enzyme-linked immunosorbent assay (ELISA) using HIV-1 gp120 antigen capture assay (ABL, Rockville, MD) with slight modification to the manufacturer's instruction. In general, gp120 standards were diluted either in rat sera (AbD Serotec, Raleigh, NC; SPF Fisher 344), rat CSF (Bioreclamation LLC., Westbury, NY; SPF Fisher 344) or brain lysate extraction buffer (Novateinbio, Woburn, MA) for standard curve. Samples were run in duplicates. Samples where duplicate absorption values differed significantly from each other were excluded.

2.4. Quantitative Real-Time Polymerase Chain Reaction (qRT-PCR) of Brain Tissues

For the assessment of viral protein expression in the Tg rat, brain tissue samples were obtained from 3 young Tg rats (2 month-old) and 4 old Tg rats (age > 1 year). Two control rat brains were used as negative controls to test the primers by regular PCR and running gel. Control brains did not show any viral protein bands on the running gel. For analysis of tat, gp120 and nef expression, 100 mg samples of frontal cortex, striatal and hippocampal tissues from each animal were used. Total cellular RNA was isolated from each tissue section using an RNeasy Lipid Tissue mini kit (Qiagen, Valencia, CA) according to the manufacturer's instructions. Synthesis of first-strand cDNA was performed using Quantitect reverse transcriptase kit (Qiagen, Hilden, Germany) and analyzed using IQ SYBR Green

PCR kit (Bio-Rad, Hercules, CA). Relative levels of specific mRNA were quantified by using the CFX96 Real-time System (Bio-Rad, Hercules, CA). Primer Sequences for tat, gp120, nef and GAPDH as well as real-time PCR conditions have been previously described (Peng, Vigorito, 2010). Primers were synthesized by RealTimePrimers (Elkins Park, PA). Samples were run in triplicate and the yield of PCR product was normalized to GAPDH. Primer efficiencies were determined in triplicate using serial 10-fold dilutions of cDNA. Primer efficiencies (E) were calculated as $E=10^{[-1/slope]}-1$; all primers used in these studies had good efficiency (E=90–110%). To control for DNA contamination, equal amounts of RNA were used without reverse transcriptase. The relative quantification of the template was then achieved using the comparative CT method, and is reported as relative transcription or the n-fold difference relative to the cDNA of the calibrator.

For the assessment of GFAP, Iba1 and CD11b expression in the Tg rat, brain tissue samples were obtained from six 1 month-old rats (3 Tg and 3WT) and ten 8–9 month-old rats (5 Tg and 5 WT). A similar procedure to the above was followed except that the synthesis of cDNA was performed using RT2 First Strand Kit (Qiagen, Hilden, Germany) and PCR was carried out with RT^2 SYBR Green qPCR Mastermix (Qiagen) using CFX96 Real-time System (Bio-Rad, Hercules, CA). All primers used were from RT2 qPCR Primer Assay (Qiagen). The relative expression levels of target mRNA were determined by ΔCt method using Actb, rplp1, and Hrpt1 for normalization. Samples were run in duplicates or PCR was repeated to confirm the results.

2.5. Statistics

Statistical significance was determined using GraphPad Instat statistical software (Version 3.0). Comparisons of immunofluorescence ratios between Tg and WT rats at different ages and in different locations were made using the nonparametric Mann-Whitney U-test since data was not always found to have a normal distribution. A p-value of <0.05 was considered significant. All data are represented as Mean (SD).

3. RESULTS

3.1. Immunofluorescence

NeuN is a sensitive and specific neuronal marker that is expressed in almost all neuronal cell types of the central and peripheral nervous system. Its high specificity for neurons makes it a good marker for studying neuronal loss (Wolf et al., 1996). NeuN Tg/WT staining count ratios were low in the striatum (ST) of both young and middle-aged HIV-1 Tg rats but were only mildly decreased in the cortex (CX) and not significantly changed in the hippocampus (HC) (Table. 1). The Tg/WT staining ratios were not significantly different statistically between the 1–3 and 7–10 month-old animals.

GFAP, an activated astrocyte marker, is considered a member of the cytoskeletal protein family and plays an important role in controlling astrocyte motility and shape by providing structural stability to astrocytic processes (Eng et al., 2000). GFAP Tg/WT staining intensity ratios were decreased in all measured regions (CX, ST, HC), and in the corpus callosum (CC) (Fig.1A and 1B, Table 1). This significantly worsened with age in the ST (Mann-

Whitney *U*-test, p=0.038) and in the CC (Mann-Whitney *U*-test, p=0.033). A similar pattern of decreasing staining ratios was noted in the CX and HC however this was not statistically significant. The loss of GFAP staining however was not consistent per age group, with some 7 month-old animals showing more GFAP staining loss than 9 month-old rats.

Ionized calcium binding adaptor molecule 1 (Iba1) is a calcium-binding protein (Imai and Kohsaka, 2002) that has an actin-bundling activity and participates in membrane ruffling and phagocytosis in activated microglia (Ohsawa et al., 2004). For Iba1 measurements, we averaged the count ratios in each animal across the ST, HC and CX considering the diffuse pattern of microglial staining across the brain, without any specific regional predilection. Iba1 Tg/WT count ratios were mildly increased in the young animals with mean ratio of 1.165 (0.288). This decreased to a ratio of 0.852 (0.148) in the middle-aged animals (Fig. 2). The difference between the two age groups was statistically significant (Mann-Whitney *U*-test, p=0.033) (Table 1).

TH is the enzyme responsible for catalyzing the conversion of the amino acid tyrosine to L-DOPA, the precursor of Dopamine; it is assumed to reflect dopaminergic neuronal integrity (Zeiss, 2005). TH Tg/WT staining intensity ratios in the striatum were decreased (mean ratio=0.76 (0.16) in young animals), and worsened with age (mean ratio=0.64 (0.21) in middle-aged animals). This was statistically significant (Mann-Whitney *U*-test, p=0.017) (Table. 1).

PCNA is a cell cycle marker associated with DNA replication and neurogenesis (Frade and Ovejero-Benito, 2015, von Bohlen und Halbach, 2011). We performed PCNA staining and evaluated the dentate gyrus and periventricular subgranular zone in newly weaned rats (1 month-old). There was no appreciable difference in PCNA staining in either location (ratios=1.18 (0.6) and 1.10 (0.7) respectively) (Fig. 3).

3.2. Viral protein level analysis

Out of 28 Tg animals that got serum gp120 levels measured, 14 animals ranging in age between 14 and 20 months had detectable levels of gp 120 (mean value= 82.8 (18.9) pg/ml). All the young animals (3–7 month-old) and four older animals (14–15 month-old) had serum levels of gp120 below the detection level of the kit (62.5 pg/ml). None of the WT rats had detectable serum levels of gp120.

Out of 17 rats that got CSF gp120 level measured, 11 had levels above the detection level of the kit (mean value = 160 (82) pg/ml).

In the 13 rats that had CSF and serum collected around the same time, 7 had detectable gp120 in the CSF (mean= 164 (95) pg/ml) with no detectable gp120 in the serum, and 2 had higher gp120 levels in the CSF than in the serum (both CSF and serum levels detectable).

Brain homogenate samples from 5 Tg animals had mean gp120 protein level of 72.7 (11.2) pg/ml. Homogenates from two of the Tg animals (8-month-old) and two WT animals (2 and 18 month-old) had gp120 protein level values below the detection limit of the kit.

3.3. Quantitative RT-PCR in brain tissues for gp120, tat and nef expression levels

The viral transcripts gp120, nef and tat were all detected by PCR followed by gel electrophoresis in the brain lysates of animals in the young and old age groups. With respect to young animals, the old animal group showed an average (in three locations) 1.47 fold increase in tat, 1.1 fold increase in gp120, and 0.77 fold decrease in nef. Although not very different from each other, the expression of nef was the highest followed by tat and then gp120.

3.4. Quantitative RT-PCR in brain tissues for GFAP, Iba1 and CD11b expression levels

We found lower GFAP mRNA expression levels in the young Tg (1 month-old) and older Tg (8–9 month-old) animals in comparison to age-matched WT animals, both in the striatum and in the hippocampus. Those differences however were not statistically significant ($p>0.05$). Iba1 and CD11b values were either slightly decreased or slightly increased however there were no statistically significant differences at either age and in either location ($p>0.05$) (Fig. 4).

4. DISCUSSION

There is currently no widely-used small animal model for HIV because mice and rats are non-permissive for HIV infection (Bieniasz and Cullen, 2000). Engineering rodents that are permissive for HIV infection is technically demanding and only a few centers in the country have mastered the production and utilization of HIV-susceptible humanized mice (Akkina, 2013, Berges and Rowan, 2011, Boska et al., 2014, Dash et al., 2012, Dash et al., 2011, Epstein et al., 2013, Gorantla et al., 2010, Zhang and Su, 2012). Despite the usefulness of the latter, they remain technically complicated to produce and sustain (Akkina, 2013, Zhang and Su, 2012), and for our purposes of developing molecular imaging biomarkers, the small brain size of the humanized mouse poses a limitation especially when lower resolution techniques such as PET imaging are used.

From prior publications we knew that the HIV-1 Tg rat manifests neurological abnormalities similar to human disease (Lashomb, Vigorito, 2009, Moran et al., 2013b, Reid, Sadowska, 2001, Vigorito, LaShomb, 2007). Brain abnormalities such as disrupted arachidonic acid metabolism (Basselin et al., 2011) and disrupted neurotransmitter systems (Guo et al., 2012, Moran, Aksenov, 2012, Sultana et al., 2010) have been reported. We've also previously described *in vivo* imaging findings in this animal model suggestive of neuropathology using both magnetic resonance imaging (MRI) and positron emission tomography (PET) (Lee et al., 2014a, Lentz et al., 2014). Although there have been previous meticulous studies examining certain aspects of brain pathology in this animal model (Repunte-Canonigo et al., 2014, Royal et al., 2012), the exact neuropathology with respect to age and whether viral proteins are expressed in the CSF have not been thoroughly characterized.

The main histopathologies we observed in the Tg rat brains at different ages involved both neuronal and glial cell lines. Age-associated neuronal loss/dysfunction was seen in the striatum but that was not significantly different between young and middle-aged animals ($p=0.33$) (Table. 1). Curiously, we noticed decreased intensity of NeuN staining in the Tg

striatal neurons compared to WT striatal neurons while at the same time no such differences could be seen involving the cortical neurons in the same slides. This suggested selective decreased NeuN immunoreactivity in the striatum. Whether this decreased immunoreactivity could partially account for the decreased cell counts in the striatum (due to difficulty detecting the borders of the cell using automated counting) is a possibility. This striatal neuronal dysfunction was further confirmed by decreased TH staining in the striatum of the Tg rats, significantly worsening with age as well, suggesting functional dopaminergic deterioration rather than just structural neuronal loss (Table. 1). This was not a surprise, considering previous studies that identified behavioral problems presumed to be due to dopaminergic dysfunction in those animals (Fitting et al., 2015, Liu et al., 2009, Moran, Aksenov, 2012, Moran, Booze, 2013b, Webb et al., 2010).

The most impressive finding, however, was progressive loss of GFAP staining, suggesting astrocytic dysfunction/damage, significantly worsening with age in the striatum and corpus callosum (Table.1, Fig.1A and 1B). This was most noticeable in the corpus callosum considering the natural higher number of astrocytes along the white matter fiber tracts in that part of the brain. Microglia, on the other hand, appeared to be slightly activated early-on (1–3 months of age), but this decreased in older animals (Fig. 2). There was still a possibility that the Tg neuropathology could be due to the presence of the transgene, affecting neurogenesis, a previously encountered problem with another small animal model of HIV, the gp120 Tg mouse (Lee et al., 2013). This is especially true considering that in the Tg rat with continuous viral protein production since birth, the age of the rat equates to time since infection in HIV+ patients. PCNA staining in newly-weaned Tg rats, however, did not differ significantly from WT animals (Fig. 3), suggesting that abnormal neurogenesis does not play an important role in the Tg neuropathology, with the latter being a progressive neurodegenerative process rather than a neurodevelopmental process.

Our results do not concur with previously published histopathology findings in the Tg rat (Repunte-Canonigo, Lefebvre, 2014) showing activation of astrocytes and microglia (increased GFAP staining) rather than astrocyte dysfunction/damage (loss of GFAP staining). In that study however, a different rat strain was used (Sprague-Dawley rather than Fischer F344) which we believe could account for the striking differences in histopathologic phenotype. This is not unusual, with multiple examples in the literature showing discrepancies in manifestations of disease between different rodents species even when expressing the same transgene (Jiang et al., 2015, Lefesvre et al., 2003, Mestre et al., 2015, Siviy et al., 2015, Stozicka et al., 2010). Unfortunately we could not test this assumption since the Sprague-Dawley Tg rat is not available commercially anymore. Another paper did not show significant differences in GFAP staining between Tg and WT rats (Royal, Zhang, 2012) however a younger age group was probably used in that study.

Our results also do not concur with the neuropathology seen in humanized HIV-1 mice which included robust inflammation reflected in GFAP and Iba-1 staining intensities (Boska, Dash, 2014, Dash, Gorantla, 2011, Epstein, Narayanasamy, 2013, Gorantla, Makarov, 2010). This however can be explained by the inherent differences between the two animal models as far as pathophysiology: the HIV humanized mouse is an immunodeficient model (NOD/scid-IL-2Rgamma(c)(null) mice) reconstituted with human hematopoietic

CD34(+) stem cells and infected with HIV, thus reflecting human HIV-1 infection more closely, with persistent viremia, profound CD4+ T lymphocyte loss and infection of human monocyte-macrophages in the meninges/perivascular spaces of the rodent brain (Boska, Dash, 2014, Epstein, Narayanasamy, 2013). The Tg rat on the other hand reflects chronic viral protein toxicity (Midde et al., 2011, Peng, Vigorito, 2010, Royal, Zhang, 2012, Vigorito et al., 2015, Wayman et al., 2015), and is closer pathologically to optimally-treated HIV+ patients than actively infected patients, as described below.

In view of what seems like a less prominent role for microglial activation in this model, we concur with previous studies asserting prolonged exposure to viral proteins as the main cause of neuropathology in the Tg rat (Midde, Gomez, 2011, Peng, Vigorito, 2010, Royal, Zhang, 2012, Vigorito, Connaghan, 2015, Wayman, Chen, 2015). Interestingly, we were able to detect serum gp120 in older but not in younger rats. This could be due to faster production of viral proteins than their degradation, or could indicate increased expression of the transgene peripherally with age. Gp120 has already been detected in the serum of older animals (Joshi et al., 2008, Reid, Sadowska, 2001) however it has not been measured in the serum of younger animals before. In addition, we detected gp120 in the CSF of both young and older animals with some Tg rats showing detectable levels of gp120 in their CSF but not in the serum or higher levels in the CSF than in the serum, suggesting local expression in the brain. This is further supported by the detection of mRNA expression of viral proteins in the brain lysates of the Tg animals, reproducing previous similar work (Peng, Vigorito, 2010, Robillard et al., 2014). In the Tg rat with continuous production of viral proteins since birth, the age of the animal would equate with time since infection in patients, further supporting the usefulness of the rat as a model of prolonged viral protein exposure.

Astrocytic vulnerability in this animal model is not completely unexpected: HIV viral protein-associated astrocytic toxicity has already been shown by many groups (Borjabad et al., 2010, Noorbakhsh et al., 2010, Torres and Noel, 2014, Wang et al., 2003, Wang et al., 2004). For example, gp120 is known to bind to astrocytes, altering the cell physiology (Chang et al., 2008), dysregulating gene expression (Borjabad, Brooks, 2010, Wang, Trillo-Pazos, 2004) and inhibiting glutamate transport (Wang, Pekarskaya, 2003) leading to further neuronal damage by excitotoxicity (Plachez et al., 2004). Tat is similarly known to cause glutamatergic dysregulation, resulting in excessive NMDA receptor activation, and secondary neuro and astrocytic toxicity (Ton and Xiong, 2013). Disruption of the expression of toll-like receptors in astrocytes exposed to tat or gp120 (El-Hage et al., 2011) and altered astrocyte morphology in SIV-infected macaques have also been described (Lee et al., 2014b).

The Tg rat brain does not reflect HIV brain pathology in advanced HIV encephalitis such as seen in the pre-ART era, since the latter was most noticeable for inflammatory changes such as macrophage infiltration, formation of multinucleated giant cells, and reactive astrogliosis (Gendelman et al., 1994, Gray et al., 1996, Lawrence and Major, 2002, Merrill and Chen, 1991). It has been previously suggested that the Tg rat can be a model for treated rather than untreated HIV+ patients (Abbondanzo and Chang, 2014, Moran, Booze, 2013a, Moran et al., 2014, Moran, Booze, 2013b, Nemeth et al., 2014, Peng, Vigorito, 2010, Vigorito, Connaghan, 2015). The current study concurs with this suggestion, since in more recent

publications examining the neuropathology in treated HIV+ patients, the classic signs of inflammation damage such as multinucleated giant cells and HIV encephalitis were lacking. Those results suggested alternative causes for the progressive neurodegeneration in this patient group (Everall et al., 2009, Gelman et al., 2013) and exposure to viral protein is one of those suggested causes (Shin and Thayer, 2013, Silverstein et al., 2012, Yadav and Collman, 2009). The subcortical pattern of neuronal damage that we see in our animals is also reminiscent of HIV damage in the post ART era (Kumar et al., 2009, Kumar et al., 2011).

One potential limitation to our study is that we did not use stereology techniques to account for possible shrinkage of the examined tissues which could compromise cell density calculations. However, we only imaged individual 10-micron thick sections at a single focal plane, which makes it impossible to obtain volumetric measurements from these image datasets. Therefore, cell counts can only be compared between matching sections and areas of interest from different brains. We also believe that as brains from all animals that were actually compared went through the same tissue preparation procedure before staining, the amount of shrinking of each brain should be the same, and cell counts in matching areas of interest from different brain sections cut at the same coronal planes should be comparable. Another limitation is that we did not directly correlate viral protein expression levels in the serum and CSF with terminal measures such as neuropathology, mRNA levels and brain lysate protein levels because the sample numbers for such correlations were too small to draw meaningful conclusions. We did however compare serum and CSF levels of gp120 measured concurrently in the same animals. We did not co-stain for viral proteins along with glial or cellular markers, however previous work has already shown expression of viral proteins such as vif and nef within the astrocytes and microglia of the Tg rat (Royal, Zhang, 2012). Finally, the use of Fischer only rather than both Fischer and Sprague-Dawley Tg rats can be considered a potential limitation since interspecies differences could not be evaluated concurrently. The Sprague-Dawley Tg rat (Harlan Inc.) however is not available commercially anymore.

5. CONCLUSIONS

We have evaluated the neuropathology of the commercially-available HIV-1 Tg rat (Fischer, F344/Hsd) as it aged, and evaluated the expression and presence of HIV viral proteins in the blood, CSF and brain tissues. The results show various glial and neuronal injury patterns however astrocytic damage seems to dominate the picture, suggesting selective vulnerability of those cells to viral proteins. With the current availability and future development of *in vivo* imaging biomarkers of disease (Lee, Reid, 2014a, Lentz, Peterson, 2014), this animal model can potentially be used in the evaluation of neuroprotective strategies that primarily target the astrocytic component of pathology as well as prolonged exposure to viral proteins. Further evaluation of the exact pathophysiology underlying the Tg astrocytic vulnerability to viral proteins remains warranted.

Acknowledgments

Sources of funding: This work was supported by the Center of Infectious Disease Imaging (CIDI), National Institutes of Health (Intramural Program).

Abbreviations

ART	antiretroviral therapy
CC	corpus callosum
CSF	cerebrospinal fluid
CX	cortex
HAART	highly active antiretroviral therapy
HAD	HIV associated dementia
HAND	HIV-1 associated neurocognitive disorders
HC	hippocampus
IACUC	Institutional Animal Care and Use Committee ()
PCNA	proliferating cell nuclear antigen
PET	positron emission tomography
ST	striatum
SVZ	subventricular zone
Tg	HIV-1 transgenic
TH	tyrosine hydroxylase
WT	wild type

References

Abbondanzo SJ, Chang SL. HIV-1 transgenic rats display alterations in immunophenotype and cellular responses associated with aging. Plos One. 2014; 9:E105256. [PubMed: 25127062]

Agrawal L, Louboutin JP, Reyes BA, Van Bockstaele EJ, Strayer DS. HIV-1 tat neurotoxicity: a model of acute and chronic exposure, and neuroprotection by gene delivery of antioxidant enzymes. Neurobiology of Disease. 2012; 45:657–670. [PubMed: 22036626]

Akkina R. New generation humanized mice for virus research: comparative aspects and future prospects. Virology. 2013; 435:14–28. [PubMed: 23217612]

Basselin M, Ramadan E, Igarashi M, Chang L, Chen M, Kraft AD, et al. Imaging upregulated brain arachidonic acid metabolism in HIV-1 transgenic rats. J Cereb Blood Flow Metab. 2011; 31:486–493. [PubMed: 20664612]

Berges BK, Rowan MR. The utility of the new generation of humanized mice to study HIV-1 infection: transmission, prevention, pathogenesis, and treatment. Retrovirology. 2011; 8:65. [PubMed: 21835012]

Bezzi P, Domercq M, Brambilla L, Galli R, Schols D, De Clercq E, et al. CXCR4-activated astrocyte glutamate release via tnfalpha: amplification by microglia triggers neurotoxicity. Nat Neurosci. 2001; 4:702–710. [PubMed: 11426226]

Bieniasz PD, Cullen BR. Multiple blocks to human immunodeficiency virus type 1 replication in rodent cells. Journal of Virology. 2000; 74:9868–9877. [PubMed: 11024113]

Borjabad A, Brooks AI, Volsky DJ. Gene expression profiles of HIV-1-infected glia and brain: toward better understanding of the role of astrocytes in HIV-1-associated neurocognitive disorders. Journal of Neuroimmune Pharmacology : The Official Journal of The Society on Neuroimmune Pharmacology. 2010; 5:44–62. [PubMed: 19697136]

Boska MD, Dash PK, Knibbe J, Epstein AA, Akhter SP, Fields N, et al. Associations between brain microstructures, metabolites, and cognitive deficits during chronic HIV-1 infection of humanized mice. Molecular Neurodegeneration. 2014; 9:58. [PubMed: 25523827]

Chang L, Wang GJ, Volkow ND, Ernst T, Telang F, Logan J, et al. Decreased brain dopamine transporters are related to cognitive deficits in HIV patients with or without cocaine abuse. Neuroimage. 2008; 42:869–878. [PubMed: 18579413]

Dash PK, Gendelman HE, Roy U, Balkundi S, Alnouti Y, Mosley RL, et al. Long-acting nanoformulated antiretroviral therapy elicits potent antiretroviral and neuroprotective responses in HIV-1-infected humanized mice. AIDS (London, England). 2012; 26:2135–2144.

Dash PK, Gorantla S, Gendelman HE, Knibbe J, Casale GP, Makarov E, et al. Loss of neuronal integrity during progressive HIV-1 infection of humanized mice. The Journal of Neuroscience : The Official Journal of the Society for Neuroscience. 2011; 31:3148–3157. [PubMed: 21368026]

Desplats P, Dumaop W, Smith D, Adame A, Everall I, Letendre S, et al. Molecular and pathologic insights from latent HIV-1 infection in the human brain. Neurology. 2013; 80:1415–1423. [PubMed: 23486877]

El-Hage N, Podhaizer EM, Sturgill J, Hauser KF. Toll-like receptor expression and activation in astroglia: differential regulation by HIV-1 tat, GP120, and Morphine. Immunological Investigations. 2011; 40:498–522. [PubMed: 21425908]

Eng LF, Ghirnikar RS, Lee YL. Glial fibrillary acidic protein: GFAP-thirty-one years (1969–2000). Neurochemical Research. 2000; 25:1439–1451. [PubMed: 11059815]

Epstein AA, Narayanasamy P, Dash PK, High R, Bathena SP, Gorantla S, et al. Combinatorial assessments of brain tissue metabolomics and histopathology in rodent models of human immunodeficiency virus infection. Journal of Neuroimmune Pharmacology : The Official Journal of the Society on Neuroimmune Pharmacology. 2013; 8:1224–1238. [PubMed: 23702663]

Everall I, Vaida F, Khanlou N, Lazzaretto D, Achim C, Letendre S, et al. Cliniconeuropathologic correlates of human immunodeficiency virus in the era of antiretroviral therapy. Journal of Neurovirology. 2009; 15:360–370. [PubMed: 20175693]

Fitting S, Booze RM, Mactutus CF. HIV-1 PROTEINS, tat and GP120, target the developing dopamine system. Current HIV Research. 2015; 13:21–42. [PubMed: 25613135]

Frade JM, Ovejero-Benito MC. Neuronal cell cycle: the neuron itself and its circumstances. Cell cycle (Georgetown, Tex). 2015; 14:712–720.

Gelman BB, Lisinicchia JG, Morgello S, Masliah E, Commins D, Achim CL, et al. Neurovirological correlation with HIV-associated neurocognitive disorders and encephalitis in a haart-era cohort. J Acquir Immune Defic Syndr. 2013; 62:487–495. [PubMed: 23242157]

Gendelman HE, Lipton SA, Tardieu M, Bukrinsky MI, Nottet HS. The neuropathogenesis of HIV-1 infection. Journal of Leukocyte Biology. 1994; 56:389–398. [PubMed: 8083614]

Gorantla S, Makarov E, Finke-Dwyer J, Castanedo A, Holguin A, Gebhart CL, et al. Links between progressive HIV-1 infection of humanized mice and viral neuropathogenesis. The American Journal of Pathology. 2010; 177:2938–2949. [PubMed: 21088215]

Gray F, Scaravilli F, Everall I, Chretien F, An S, Boche D, et al. Neuropathology of early HIV-1 infection. Brain Pathology (Zurich, Switzerland). 1996; 6:1–15.

Guo M, Bryant J, Sultana S, Jones O, Royal W 3rd. Effects of vitamin a deficiency and opioids on parvalbumin + interneurons in the hippocampus of the HIV-1 Transgenic Rat. Current HIV Research. 2012; 10:463–468. [PubMed: 22591370]

Hu S, Sheng WS, Lokensgard JR, Peterson PK, Rock RB. Preferential sensitivity of human dopaminergic neurons to GP120-induced oxidative damage. Journal of Neurovirology. 2009; 15:401–410. [PubMed: 20175694]

Imai Y, Kohsaka S. Intracellular signaling in M-CSF-induced microglia activation: role of IBA1. Glia. 2002; 40:164–174. [PubMed: 12379904]

Jiang B, Deng Y, Suen C, Taha M, Chaudhary KR, Courtman DW, et al. Marked strain-specific differences in the SU5416 rat model of severe pulmonary arterial hypertension. American Journal of Respiratory Cell and Molecular Biology. 2015

Joshi PC, Raynor R, Fan X, Guidot DM. HIV-1-transgene expression in rats decreases alveolar macrophage zinc levels and phagocytosis. American Journal of Respiratory Cell and Molecular Biology. 2008; 39:218–226. [PubMed: 18314538]

Kovalevich J, Langford D. Neuronal toxicity in HIV CNS disease. Future Virology. 2012; 7:687–698. [PubMed: 23616788]

Kumar AM, Fernandez JB, Singer EJ, Commins D, Waldrop-Valverde D, Ownby RL, et al. Human immunodeficiency virus type 1 in the central nervous system leads to decreased dopamine in different regions of postmortem human brains. Journal of Neurovirology. 2009; 15:257–274. [PubMed: 19499455]

Kumar AM, Ownby RL, Waldrop-Valverde D, Fernandez B, Kumar M. Human immunodeficiency virus infection in the CNS and decreased dopamine availability: relationship with neuropsychological performance. Journal of Neurovirology. 2011

Lashomb AL, Vigorito M, Chang SL. Further characterization of the spatial learning deficit in the human immunodeficiency virus-1 transgenic rat. Journal of Neurovirology. 2009; 15:14–24. [PubMed: 19085205]

Lawrence DM, Major EO. HIV-1 and the brain: connections between HIV-1-associated dementia, neuropathology and neuroimmunology. Microbes and Infection / Institut Pasteur. 2002; 4:301–308. [PubMed: 11909740]

Lee DE, Reid WC, Ibrahim WG, Peterson KL, Lentz MR, Maric D, et al. Imaging dopaminergic dysfunction as a surrogate marker of neuropathology in a small-animal model of HIV. Molecular Imaging. 2014A; 13:1–10. [PubMed: 24824853]

Lee KM, Chiu KB, Renner NA, Sansing HA, Didier PJ, Maclean AG. Form follows function: astrocyte morphology and immune dysfunction in SIV neuroaids. Journal of Neurovirology. 2014B; 20:474–484. [PubMed: 24970236]

Lee MH, Amin ND, Venkatesan A, Wang T, Tyagi R, Pant HC, et al. Impaired neurogenesis and neurite outgrowth in an HIV-GP120 transgenic model is reversed by exercise Via BDNF production and CDK5 regulation. Journal of Neurovirology. 2013; 19:418–431. [PubMed: 23982957]

Lefesvre P, Attema J, Van Bekkum D. Pharmacogenetic heterogeneity of transgene expression in muscle and tumours. BMC Pharmacology. 2003; 3:11. [PubMed: 12943556]

Lentz MR, Peterson KL, Ibrahim WG, Lee DE, Sarlls J, Lizak MJ, et al. Diffusion tensor and volumetric magnetic resonance measures as biomarkers of brain damage in a small animal model of HIV. Plos One. 2014; 9:E105752. [PubMed: 25144656]

Liu X, Chang L, Vigorito M, Kass M, Li H, Chang SL. Methamphetamine-induced behavioral sensitization is enhanced in the HIV-1 transgenic rat. Journal of Neuroimmune Pharmacology : The Official Journal of the Society on Neuroimmune Pharmacology. 2009; 4:309–316. [PubMed: 19444617]

Mcarthur JC, Haughey N, Gartner S, Conant K, Pardo C, Nath A, et al. Human immunodeficiency virus-associated dementia: an evolving disease. Journal of Neurovirology. 2003; 9:205–221. [PubMed: 12707851]

Mcarthur JC, Steiner J, Sacktor N, Nath A. Human immunodeficiency virus-associated neurocognitive disorders: mind the GAP. Annals of Neurology. 2010; 67:699–714. [PubMed: 20517932]

Merrill JE, Chen IS. HIV-1, macrophages, glial cells, and cytokines in aids nervous system disease. Faseb Journal : Official Publication of the Federation of American Societies for Experimental Biology. 1991; 5:2391–2397. [PubMed: 2065887]

Mestre H, Ramirez M, Garcia E, Martinon S, Cruz Y, Campos MG, et al. Lewis, Fischer 344, and sprague-dawley rats display differences in lipid peroxidation, motor recovery, and rubrospinal tract preservation after spinal cord injury. Frontiers in Neurology. 2015; 6:108. [PubMed: 26029162]

Midde NM, Gomez AM, Harrod SB, Zhu J. Genetically expressed HIV-1 viral proteins attenuate nicotine-induced behavioral sensitization and alter mesocorticolimbic ERK and CREB signaling in rats. Pharmacology, Biochemistry, and Behavior. 2011; 98:587–597.

Mocchetti I, Bachis A, Avdoshina V. Neurotoxicity of human immunodeficiency virus-1: viral proteins and axonal transport. Neurotox Res. 2011

Moran LM, Aksenov MY, Booze RM, Webb KM, Mactutus CF. Adolescent HIV-1 transgenic rats: evidence for dopaminergic alterations in behavior and neurochemistry revealed by methamphetamine challenge. Current HIV Research. 2012; 10:415–424. [PubMed: 22591365]

Moran LM, Booze RM, Mactutus CF. Time and time again: temporal processing demands implicate perceptual and gating deficits in the HIV-1 transgenic rat. Journal of Neuroimmune Pharmacology : the Official Journal of the Society on Neuroimmune Pharmacology. 2013A; 8:988–997. [PubMed: 23690140]

Moran LM, Booze RM, Mactutus CF. Modeling deficits in attention, inhibition, and flexibility in hand. Journal of Neuroimmune Pharmacology : the Official Journal of the Society on Neuroimmune Pharmacology. 2014; 9:508–521. [PubMed: 24764039]

Moran LM, Booze RM, Webb KM, Mactutus CF. Neurobehavioral alterations in HIV-1 transgenic rats: evidence for dopaminergic dysfunction. Exp Neurol. 2013B; 239:139–147. [PubMed: 23063600]

Nemeth CL, Glasper ER, Harrell CS, Malviya SA, Otis JS, Neigh GN. Meloxicam blocks neuroinflammation, but not depressive-like behaviors, in HIV-1 transgenic female rats. Plos One. 2014; 9:E108399. [PubMed: 25271421]

Noorbakhsh F, Ramachandran R, Barsby N, Ellestad KK, Leblanc A, Dickie P, et al. Microrna profiling reveals new aspects of HIV neurodegeneration: caspase-6 regulates astrocyte survival. Faseb Journal : Official Publication of the Federation of American Societies for Experimental Biology. 2010; 24:1799–1812. [PubMed: 20097875]

Ohsawa K, Imai Y, Sasaki Y, Kohsaka S. Microglia/Macrophage-specific protein iba1 binds to fimbrin and enhances its actin-bundling activity. J Neurochem. 2004; 88:844–856. [PubMed: 14756805]

Peng J, Vigorito M, Liu X, Zhou D, Wu X, Chang SL. The HIV-1 transgenic rat as a model for HIV-1 infected individuals on haart. Journal of Neuroimmunology. 2010; 218:94–101. [PubMed: 19913921]

Plachez C, Martin A, Guiramand J, Recasens M. Astrocytes repress the neuronal expression of glast and GLT glutamate transporters in cultured hippocampal neurons from embryonic rats. Neurochem Int. 2004; 45:1113–1123. [PubMed: 15337311]

Radja F, Kay DG, Albrecht S, Jolicoeur P. Oligodendrocyte-specific expression of human immunodeficiency virus type 1 nef in transgenic mice leads to vacuolar myelopathy and alters oligodendrocyte phenotype in vitro. Journal of Virology. 2003; 77:11745–11753. [PubMed: 14557659]

Reid W, Sadowska M, Denaro F, Rao S, Foulke J Jr, Hayes N, et al. An HIV-1 Transgenic rat that develops HIV-related pathology and immunologic dysfunction. Proc Natl Acad Sci U S A. 2001; 98:9271–9276. [PubMed: 11481487]

Repunte-Canonigo V, Lefebvre C, George O, Kawamura T, Morales M, Koob GF, et al. Gene expression changes consistent with neuroaids and impaired working memory in HIV-1 transgenic rats. Molecular Neurodegeneration. 2014; 9:26. [PubMed: 24980976]

Robillard KR, Hoque MT, Bendayan R. Expression of ATP-binding cassette membrane transporters in a HIV-1 transgenic rat model. Biochemical and Biophysical Research Communications. 2014; 444:531–536. [PubMed: 24472536]

Royal W 3rd, Zhang L, Guo M, Jones O, Davis H, Bryant JL. Immune activation, viral gene product expression and neurotoxicity in the HIV-1 transgenic rat. Journal of Neuroimmunology. 2012; 247:16–24. [PubMed: 22503372]

Shin AH, Thayer SA. Human immunodeficiency virus-1 protein tat induces excitotoxic loss of presynaptic terminals in hippocampal cultures. Molecular and Cellular Neurosciences. 2013; 54:22–29. [PubMed: 23267846]

Silverstein PS, Shah A, Weemhoff J, Kumar S, Singh DP, Kumar A. HIV-1 GP120 and drugs of abuse: interactions in the central nervous system. Current HIV Research. 2012; 10:369–383. [PubMed: 22591361]

Siviy SM, McDowell LS, Eck SR, Turano A, Akopian G, Walsh JP. Effects of amphetamine on striatal dopamine release, open-field activity, and play in Fischer 344 and sprague-dawley rats. Behavioural Pharmacology. 2015; 26:720–732. [PubMed: 26397758]

Stozicka Z, Zilka N, Novak P, Kovacech B, Bugos O, Novak M. Genetic background modifies neurodegeneration and neuroinflammation driven by misfolded human tau protein in rat model of tauopathy: implication for immunomodulatory approach to alzheimer's disease. Journal of Neuroinflammation. 2010; 7:64. [PubMed: 20937161]

Sultana S, Li H, Puche A, Jones O, Bryant JL, Royal W. Quantitation of parvalbumin+ neurons and human immunodeficiency virus type 1 (HIV-1) regulatory gene expression in the HIV-1 transgenic rat: effects of vitamin a deficiency and morphine. Journal of Neurovirology. 2010; 16:33–40. [PubMed: 20113193]

Ton H, Xiong H. Astrocyte dysfunctions and HIV-1 neurotoxicity. Journal of AIDS & Clinical Research. 2013; 4:255. [PubMed: 24587966]

Torres L, Noel RJ Jr. Astrocytic expression of HIV-1 viral protein r in the hippocampus causes chromatolysis, synaptic loss and memory impairment. Journal of Neuroinflammation. 2014; 11:53. [PubMed: 24655810]

Vigorito M, Connaghan KP, Chang SL. The HIV-1 transgenic rat model of neuroHIV. Brain, Behavior, and Immunity. 2015

Vigorito M, Lashomb AL, Chang SL. Spatial learning and memory in HIV-1 transgenic rats. Journal of Neuroimmune Pharmacology : The Official Journal of the Society on Neuroimmune Pharmacology. 2007; 2:319–328. [PubMed: 18040850]

von Bohlen und Halbach O. Immunohistological markers for proliferative events, gliogenesis, and neurogenesis within the adult hippocampus. Cell and Tissue Research. 2011; 345:1–19. [PubMed: 21647561]

Wang Z, Pekarskaya O, Bencheikh M, Chao W, Gelbard HA, Ghorpade A, et al. Reduced expression of glutamate transporter eaat2 and impaired glutamate transport in human primary astrocytes exposed to HIV-1 or GP120. Virology. 2003; 312:60–73. [PubMed: 12890621]

Wang Z, Trillo-Pazos G, Kim SY, Canki M, Morgello S, Sharer LR, et al. Effects of human immunodeficiency virus type 1 on astrocyte gene expression and function: potential role in neuropathogenesis. Journal of Neurovirology. 2004; 10(Suppl 1):25–32. [PubMed: 14982736]

Wayman WN, Chen L, Persons AL, Napier TC. Cortical consequences of HIV-1 tat exposure in rats are enhanced by chronic cocaine. Current HIV Research. 2015; 13:80–87. [PubMed: 25760043]

Webb KM, Aksenov MY, Mactutus CF, Booze RM. Evidence for developmental dopaminergic alterations in the human immunodeficiency virus-1 transgenic rat. Journal of Neurovirology. 2010; 16:168–173. [PubMed: 20337512]

Wolf HK, Buslei R, Schmidt-Kastner R, Schmidt-Kastner PK, Pietsch T, Wiestler OD, et al. Neun: a useful neuronal marker for diagnostic histopathology. The Journal of Histochemistry and Cytochemistry : Official Journal of the Histochemistry Society. 1996; 44:1167–1171. [PubMed: 8813082]

Yadav A, Collman RG. CNS inflammation and macrophage/microglial biology associated with HIV-1 infection. Journal of Neuroimmune Pharmacology : the Official Journal of the Society on Neuroimmune Pharmacology. 2009; 4:430–447. [PubMed: 19768553]

Zeiss CJ. Neuroanatomical phenotyping in the mouse: the dopaminergic system. Veterinary Pathology. 2005; 42:753–773. [PubMed: 16301571]

Zhang L, Su L. HIV-1 Immunopathogenesis in humanized mouse models. Cellular & Molecular Immunology. 2012; 9:237–244. [PubMed: 22504952]

HIGHLIGHTS

1. Astrocytic damage dominates the neuropathology in HIV-1 Tg rats
2. No neurogenesis abnormalities in the Tg rat suggesting neurodegenerative process
3. CSF gp120 levels higher than serum in some Tg rats suggesting local production

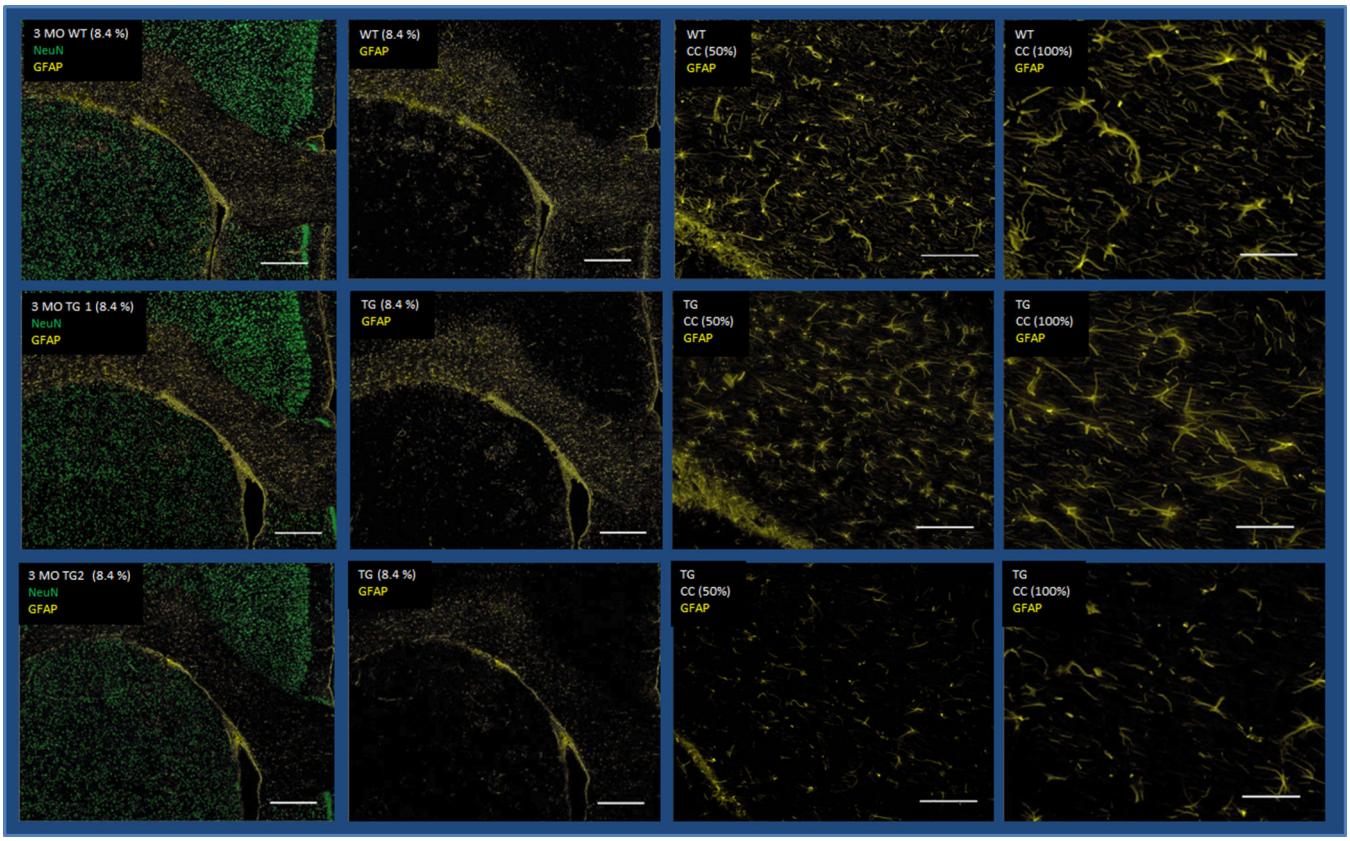

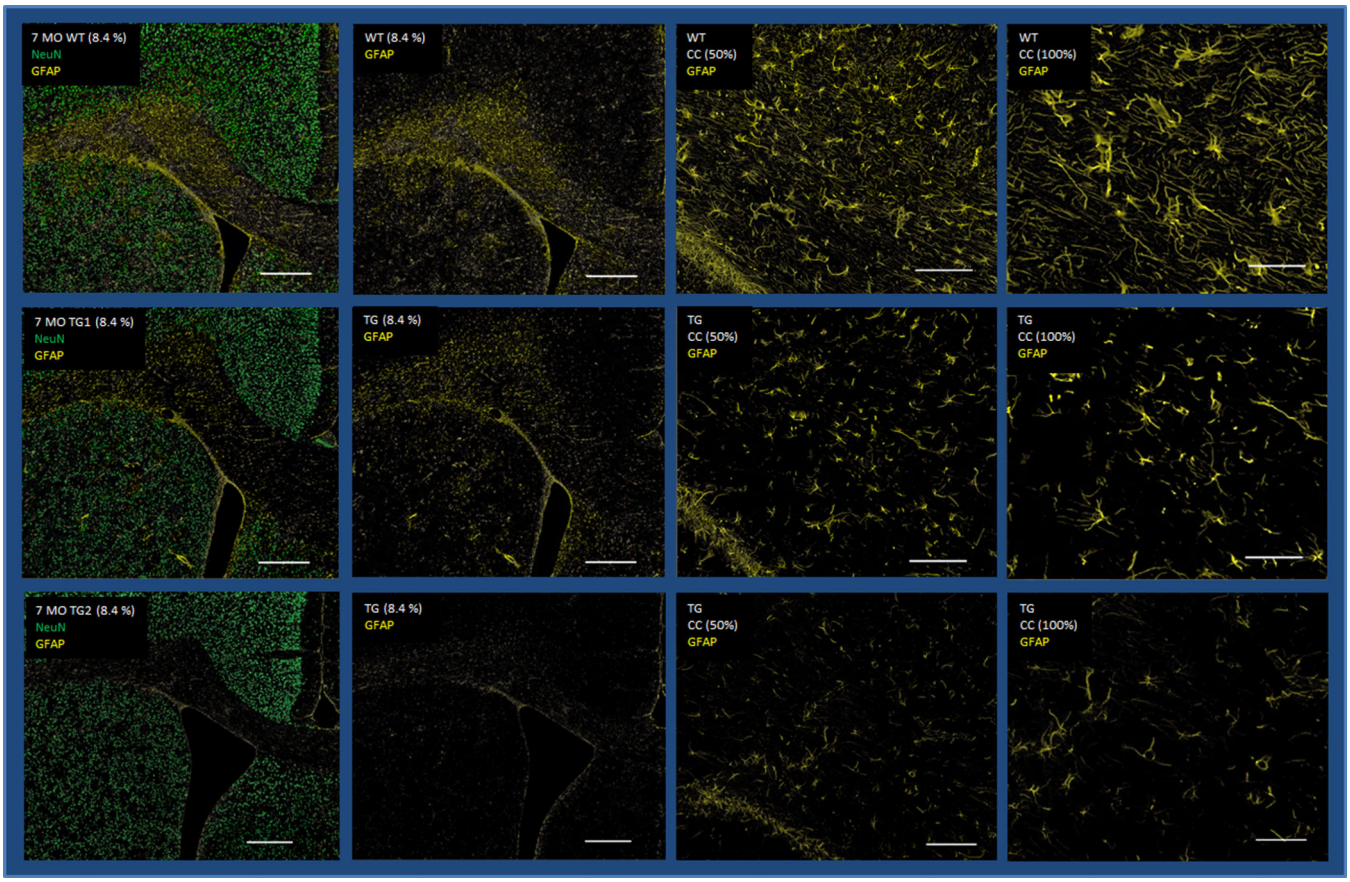

Fig. 1.

(A) Brain sections of one 3-month-old WT (upper row) and two age-matched Tg rats (middle and lower rows), encompassing parts of the cortex (CX), striatum (ST), and corpus callosum (CC) stained with NeuN (green) and GFAP (yellow) (first and second columns: 8.4× magnification, scale bar: 500μm; third and fourth columns: 50× magnification, scale bar: 100μm). (B) Brain sections of one 7-month-old WT (upper row) and two age-matched Tg rats (middle and lower rows), encompassing parts of the cortex (CX), striatum (ST), and corpus callosum (CC) stained with NeuN (green) and GFAP (yellow) (first and second columns: 8.4× magnification, scale bar: 500μm; third and fourth columns: 50× magnification, scale bar: 100μm). Decreased GFAP staining is seen in at least one of the two 3 month-old Tg animals (lower row) however is more obvious in the 7 month-old rats.

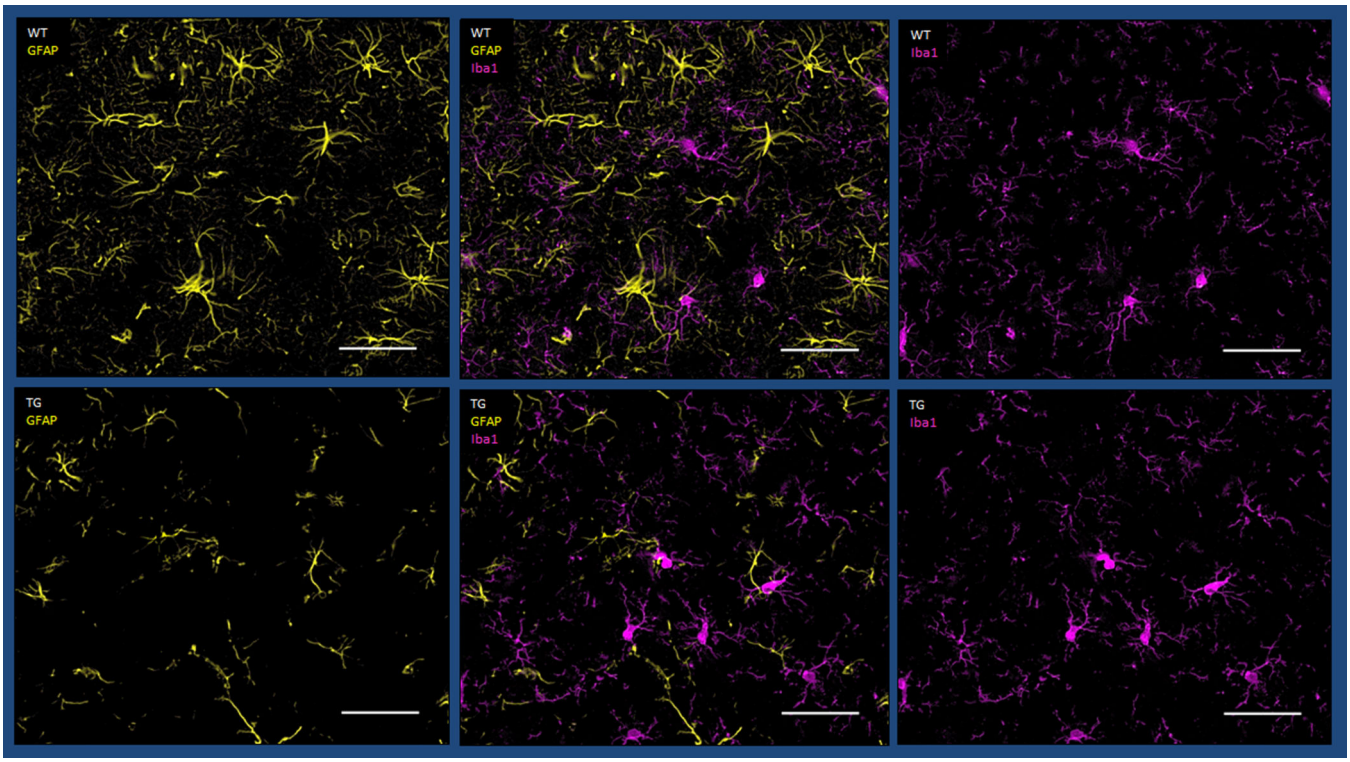

Fig. 2.

Brain sections of 7-month-old WT (upper row) and age-matched Tg (lower row) rats, at the level of the striatum (magnification 100×, Scale bar: 50μm). Decreased GFAP staining is seen in the Tg compared to WT rat however Iba1 staining appears comparable.

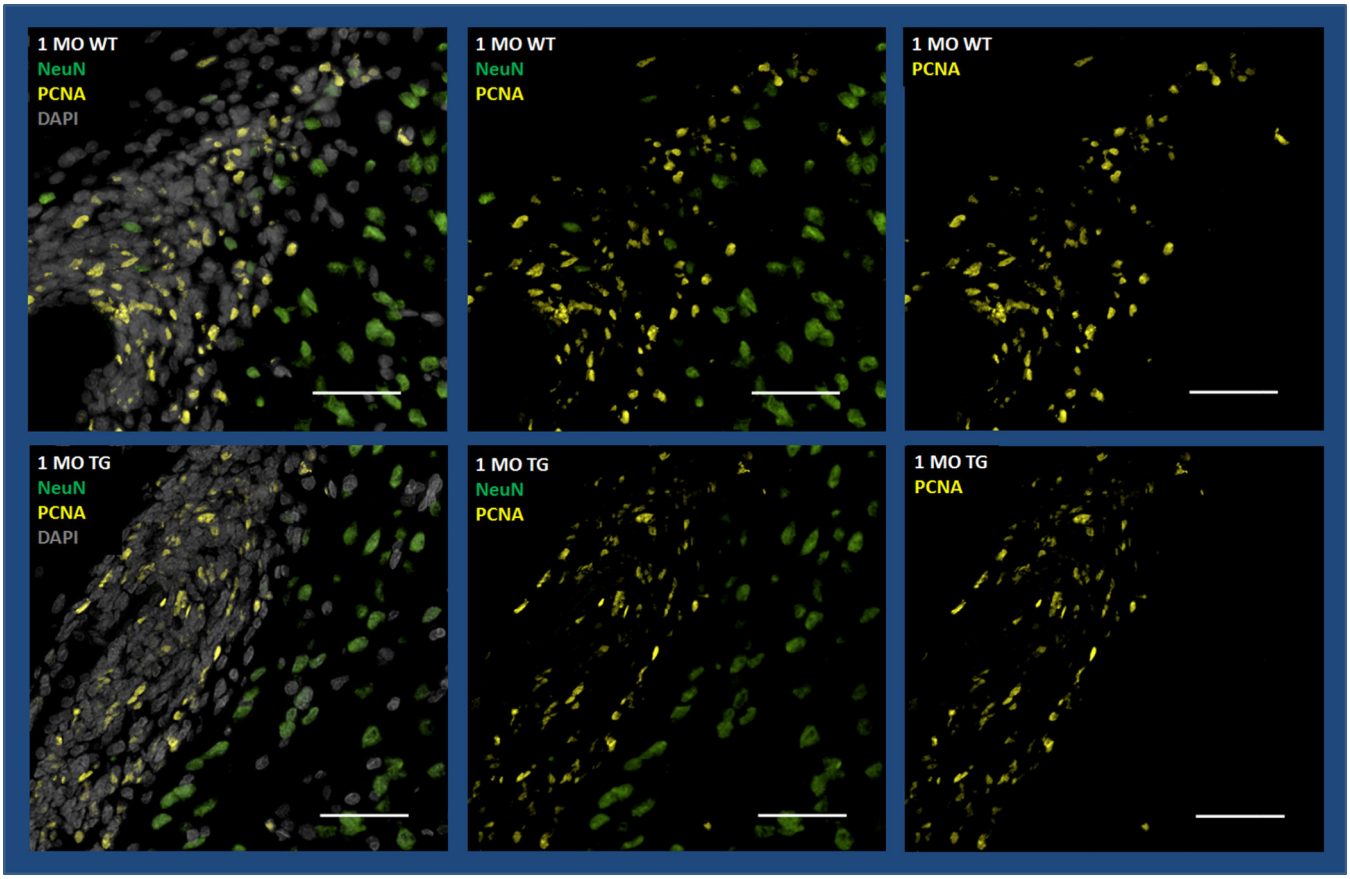

Fig. 3.

PCNA staining (yellow) in the subventricular zone (SVZ) in 1 month-old WT and Tg rat brains is comparable suggesting preserved neurogenesis in the Tg rat despite the presence of the transgene (magnification 100×, Scale bar: 50μm). Additional stains include DAPI (gray) and NeuN (green).

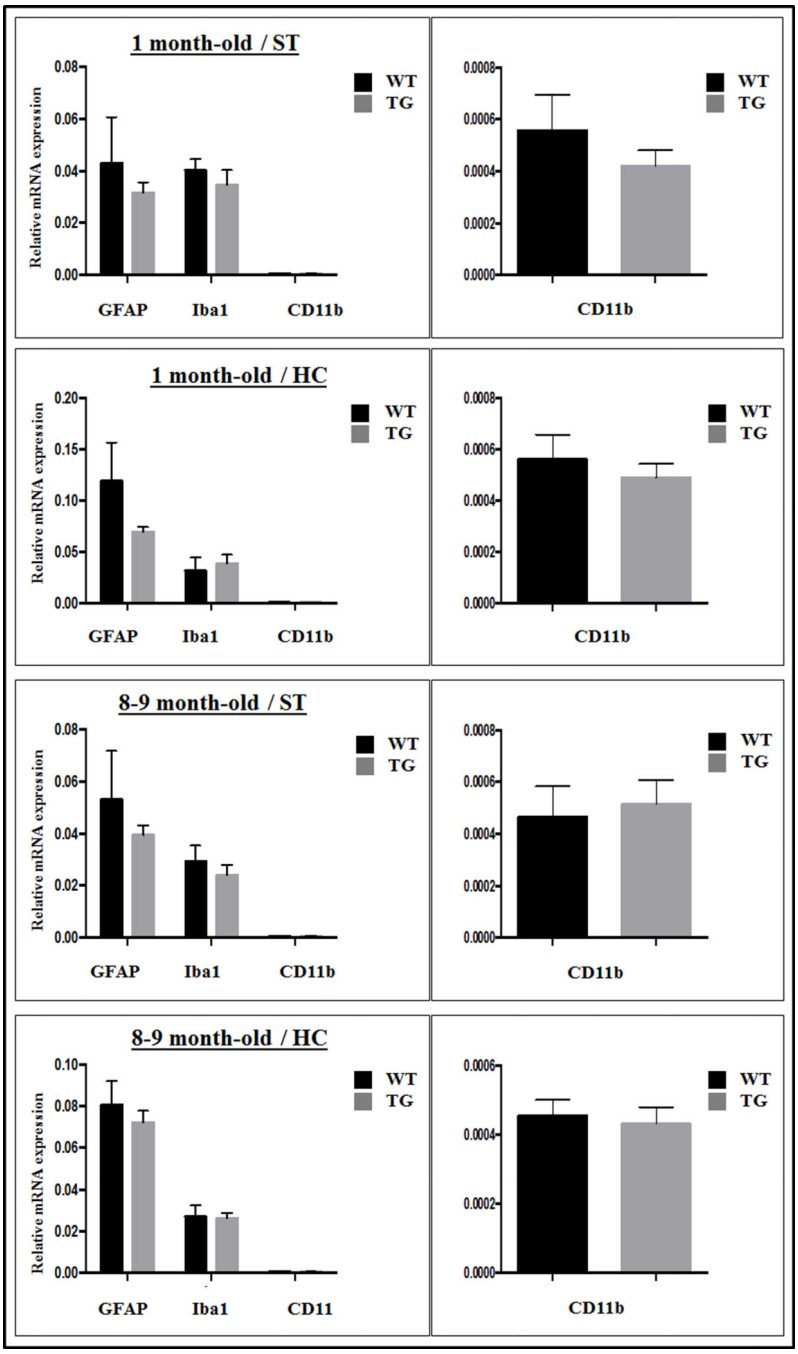

Fig. 4.

Relative mRNA expression levels of GFAP, Iba1 and CD11b in striatal (ST) and hippocampal (HC) tissues derived from 1 month-old (n= 3) and 8–9 month-old (n=5) Tg and WT rats. Although GFAP expression was generally lower in the Tg compared to WT rats, those differences were not statistically significant in either age group. Values for CD11b are re-plotted separately using a different scale for better appreciation. Error bars represent standard deviation values.

Table. 1

Quantitative staining results: Values represent Tg/WT ratios (standard deviation) of cell densities or staining intensities obtained on animal sections stained concurrently. Young animals are 1–3 month-old (8 Tg and 6 WT) and middle-aged animals are 7–9 month-old (6 Tg and 5 WT). Evaluated regions include cortex (CX), striatum (ST), hippocampus (HC) and corpus callosum (CC).

STAIN		Average of Transgenic/Wild type staining ratios			
		Striatum	**Cortex**	**Hippocampus**	**Corpus callosum**
NeuN (cells/mm2)	Young	0.615 (0.243)	0.805 (0.13)	0.967 (0.100)	-
	Middle-aged	0.498 (0.224)	0.79 (0.131)	1.089 (0.276)	-
	p-value	0.332	0.952	0.218	-
GFAP (Total intensity/mm2)	Young	0.623 (0.501)	0.674 (0.322)	0.779 (0.764)	0.738 (0.383)
	Middle-aged	0.380(0.421)	0.753 (0.796)	0.609 (0.764)	0.318 (0.183)
	p-value	**0.038***	0.834	0.352	**0.033***
Iba1 (cells/mm2)	Young	1.165(0.288)			-
	Middle-aged	0.852 (0.148)			-
	p-value	**0.033***			-
Tyrosine hydroxylase (Total intensity/mm2)	Young	0.754 (0.156)	-	-	-
	Middle-aged	0.643 (0.209)	-	-	-
	p-value	**0.0168***	-	-	-